An Integrated Approach to Dynamic Analysis of Railroad Track Transitions Behavior

D. Mishra, Y. Qian, E. Tutumluer
University of Illinois at Urbana-Champaign, Urbana, IL, USA

H. Huang
Pennsylvania State University, Altoona, PA, USA

ABSTRACT: Railway transitions like bridge approaches experience differential movements due to differences in track stiffness, track damping characteristics, ballast settlement from fouling and/or degradation, as well as fill and subgrade settlement. Proper understanding of this phenomenon requires the integration of field instrumentation with analytical and numerical modeling. This paper introduces an integrated approach to dynamic analysis of the railway track transitions behavior using field instrumentation, analytical modeling, as well as numerical simulations using the Discrete Element Method (DEM). Track response data from instrumented bridge approaches were used to calibrate a fully-coupled 3-dimensional track dynamic model. Loading profiles generated from this model were then used as input for a discrete element based program to predict individual particle accelerations within the ballast layer. The importance of modeling the ballast layer as a particulate medium has been highlighted, and the particle to particle nature of load transfer within the ballast layer has been demonstrated.

1 INTRODUCTION

Railway track transitions present a significant challenge as far as maintenance of track profile is concerned. Differences in track system stiffness and/or damping characteristics, settlement of the ballast layer due to degradation and/or fouling, and settlement of the subgrade and/or fill layers are some of the factors commonly reported as mechanisms contributing to the differential movement at track transitions. Proper understanding of different mechanisms contributing to this phenomenon requires the combined application of field instrumentation with analytical and numerical track modeling. This paper introduces an integrated approach to dynamic modeling of railway track transitions through field instrumentation and analytical and numerical modeling.

2 FIELD INSTRUMENTATION OF SELECTED TRACK TRANSITIONS

A research study sponsored by the Federal Railroad Administration is currently being carried out at the University of Illinois with the overall objective of identifying and mitigating different factors contributing to the differential movement at railway transitions. Several problematic track transitions have been instrumented under the scope of the current study to monitor the track response under loading. Data from the instrumented track transitions are being used to calibrate different analytical and numerical models to predict the dynamic track behavior under train loading. A brief description of the instrumentation used in the current study is first presented in sections below.

2.1 *Instrumentation Details*

The instrumentation used in the current study comprised multidepth deflectometers (MDDs) for measuring track substructure layer deformations, and strain gauges mounted on the rail for measuring the vertical wheel loads and tie support reactions. The MDD technology was first developed in South Africa in the early 1980s to measure individual layer deformations in highway pavements (Scullion et al., 1989). MDDs typically consist of up to six linear variable differential transformers (LVDTs) installed vertically at preselected depths in a small-diameter (hole diameter = 45 mm for the current study) hole to measure the deformation of individual track layers with respect to a fixed anchor buried deep in the ground (DeBeer et al., 1989). More details on the operation principle of MDDs can be found elsewhere (DeBeer et al., 1989; Mishra et al., 2012). It is noteworthy that the use of MDDs to monitor railway track performance has been extensively pursued in

South Africa (Grabe et al., 2005, 2010; Priest et al., 2010; Vorster & Grabe, 2013).

Figure 1 shows the schematic of an MDD system with five modules/LVDTs each installed at track substructure layer interfaces. Individual LVDTs are placed at different depths inside the borehole to measure the deflections at (1) top of ballast layer, (2) top of fouled ballast layer, (3) top of embankment fill layer 1, (4) top of embankment fill layer 2, and (5) top of the subgrade layer, respectively. The approach fill layer or the subgrade as indicated in Figure 1 can conceptually be divided into two separate segments: "deformable" and "non-deformable", respectively. The MDD anchor is fixed at a depth that is assumed to be in a "non-deformable" subgrade (or approach fill). Note that the deformations of substructure layers measured using the MDD technology is dependent on the assumption that the anchor is located in a non-deformable layer, and does not undergo any elastic or permanent deformation. Accordingly, for accurate measurement of layer deformations using the MDD approach, it is important to ensure that the anchor is located sufficiently below the track level.

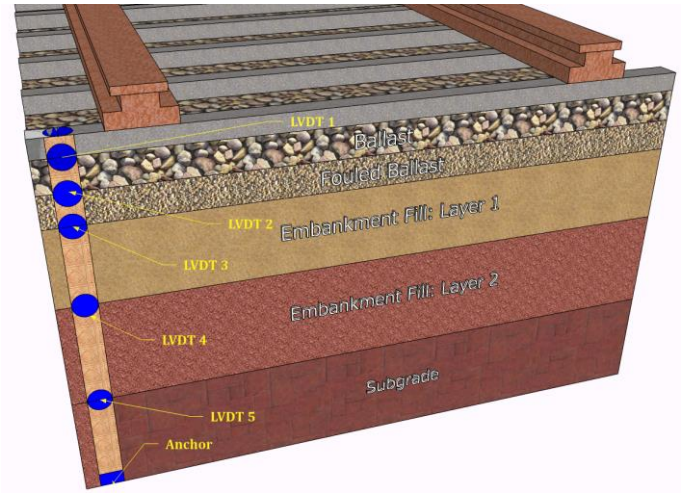

Figure 1. Schematic of Track Structure Showing Positions of Individual LVDT Modules along the MDD Hole

Note that due to the presence of overhead catenary cables, the boreholes for MDD installation in the current study could not be drilled deeper than 3.0 m below the top of the tie. Accordingly, the MDD anchor was placed at a depth of 3.0 m below the top of the crosstie. However, this is likely to be sufficient to ensure the "rigidity" of the anchor, as the instrumented sites have been in service for more than 100 years. Accordingly, the embankment fill and subgrade layers have likely been fully consolidated, resulting in no significant elastic or plastic deformations.

2.2 *Track Substructure Layer Configuration*

The track substructure layer profile was determined during the drilling by visual classification of the soil coming out of the drilled hole. The drilling was carried out in small (25-50 mm) increments to ensure that the depths of substructure layer interfaces could be identified with reasonable accuracy. The positions of individual MDD modules correspond to changes in the track substructure layer interfaces as determined during the drilling process. Figure 2 shows the layer profile established during the instrumentation of one of the bridge approaches. Note that the term "fouled ballast" has been used to indicate the section of ballast layer that was contaminated with fine materials from underlying layers. Accordingly, this terminology is not intended to make references to the quality of ballast material used in the instrumented approaches.

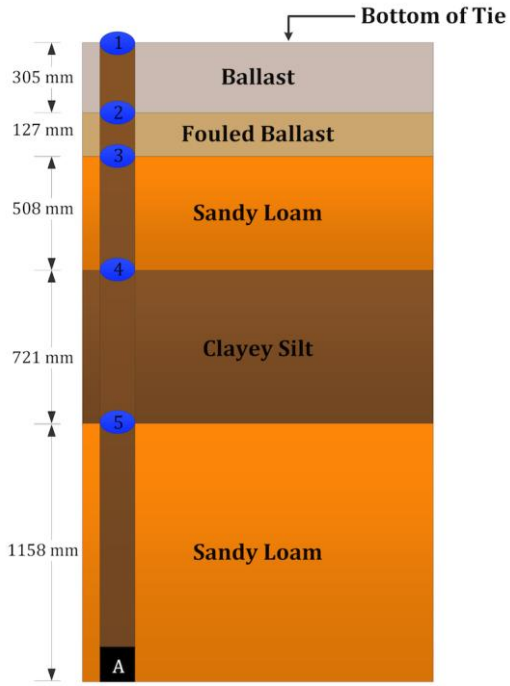

Figure 2. Substructure Layer Profile for Instrumented Track Section Analyzed in this Paper. The numbers 1 through 5 indicate the positions of the LVDTs installed along the hole for measuring individual substructure layer deformations

In addition to the MDDs, strain gauges were also installed on the rail to measure the vertical wheel load and tie reaction forces. A total of eight (8) strain gauges (two sets of four, constituting two different Wheatstone bridges) were installed next to each MDD hole.

2.3 *Periodic Monitoring and Data Acquisition*

Two types of data are currently being collected from the instrumented bridge approaches to monitor and evaluate their performances. To monitor the permanent deformation accumulations in individual

track substructure layers, "offset measurements" are being collected from the instruments at one to two week intervals. Additionally, transient (recoverable) deformations are also being collected for each approach under train loading at two to three month intervals. Figure 3 shows presents the transient data collected from one of the instrumented bridge approaches during the passage of an Amtrak Acela express passenger train.

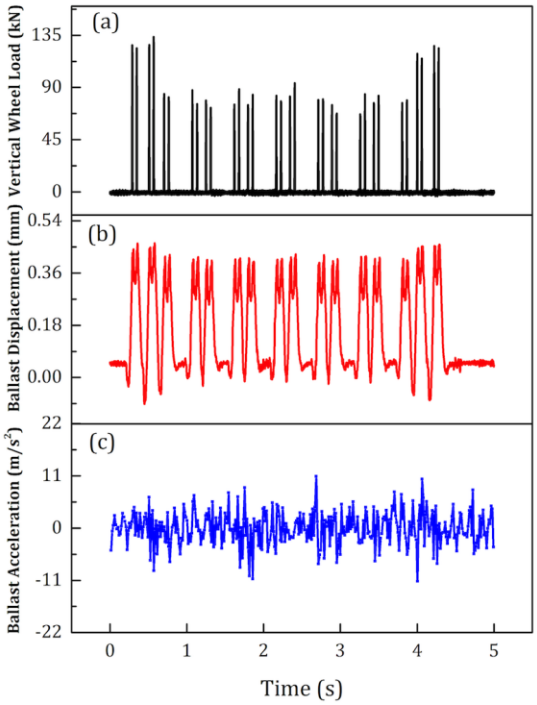

Figure 3. Field Measured Values for (a) Vertical Wheel Load Applied on Top of Rail, (b) Ballast Layer Deflection, and (c) Ballast Layer Acceleration

A typical Acela express train comprises two power cars (one at either end) separated by six passenger cars. This configuration of the train is clearly reflected by the vertical wheel load values registered by the strain gauges installed on the rail (see Figure 3-a). The heavier power cars clearly apply higher loads on the rail compared to the passenger cars. Moreover, the peaks corresponding to individual axles (32 in total) passing over the instrumentation location is clearly evident from the graph. Figure 3-b shows the transient deformations recorded by the top LVDT under the passage of the same train. Note that the top LVDT was mounted within the concrete crosstie, just above the top of the ballast layer. As the concrete crosstie is rigid, and does not undergo any deformation under loading, the deformations recorded by the top LVDT can be assumed to represent the deformation within the ballast layer. Figure 3-b shows the layer acceleration values calculated for the ballast layer from the LVDT-recorded transient deformations.

3 A FULLY COUPLED 3-DIMENSIONAL MODEL FOR DYNAMIC ANALYSIS OF TRACKS

As already mentioned, the integrated approach presented in this paper presents the combined application of field-instrumentation along with analytical and numerical track modeling. Wheel load and transient layer deformation values collected from the instrumented bridge approaches under train loading were first used to calibrate a fully coupled three dimensional train-track-soil model developed by Huang et al. (2013). This model is a modified version of the 3-D Sandwich model developed by Huang et al. (2010), and characterizes the subgrade as a three-dimensional plane stress finite element mesh. Additionally, the rail is modeled as an Euler beam discretely supported at points corresponding to the tie locations. Each railpad, tie, and ballast system is modeled using a combination of mass, spring, and damper. The train is modeled as a simplified Type I vehicle with both primary and secondary suspensions having 10 degrees of freedom. More details on the analytical model used to model the track behavior can be found elsewhere (Huang et al., 2013). Figure 4 shows a schematic representation of the dynamic track model used in the current study.

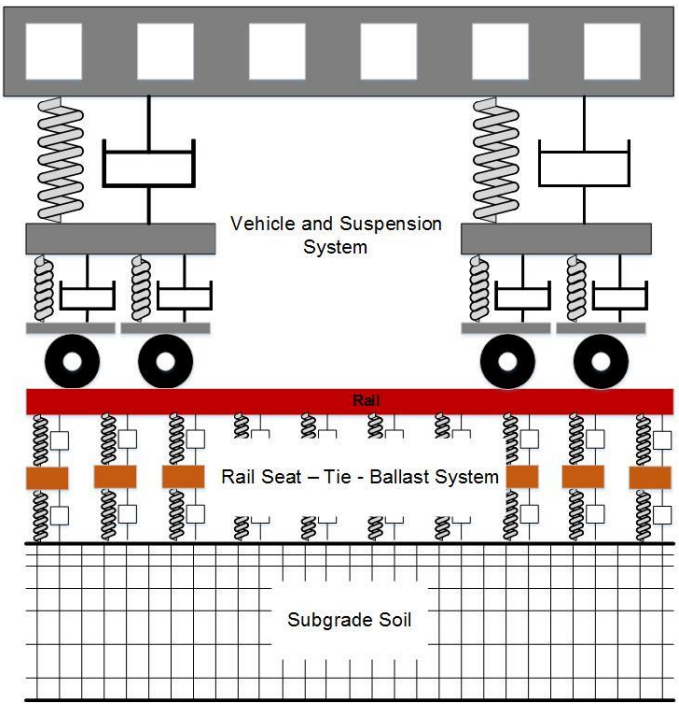

Figure 4. Schematic Representation of Fully-Coupled 3D Track Model used in the Current Study. Model Developed by Huang et al. (2013).

The track substructure profile presented in Figure 2 was used in the dynamic track model to model all the layers underlying the ballast layer. Accordingly, the modulus values for these layers were adjusted until the layer deformations predicted by the analytical model closely corresponded to those measured in

the field. This final combination of layer modulus values was then used to determine the load levels transmitted to the ballast layer. Figure 5 shows the load levels applied on top of the ballast layer, as predicted from the analytical track model. As expected, the load levels on top of the ballast are significantly lower than those measured on the rail using strain gauges. Moreover, the analytical track model also predicts higher load levels corresponding to the power car compared to the passenger cars. The maximum load level applied on the ballast layer is 23.3 kN, which is approximately 17% of the maximum load value measure on the rail (134 kN).

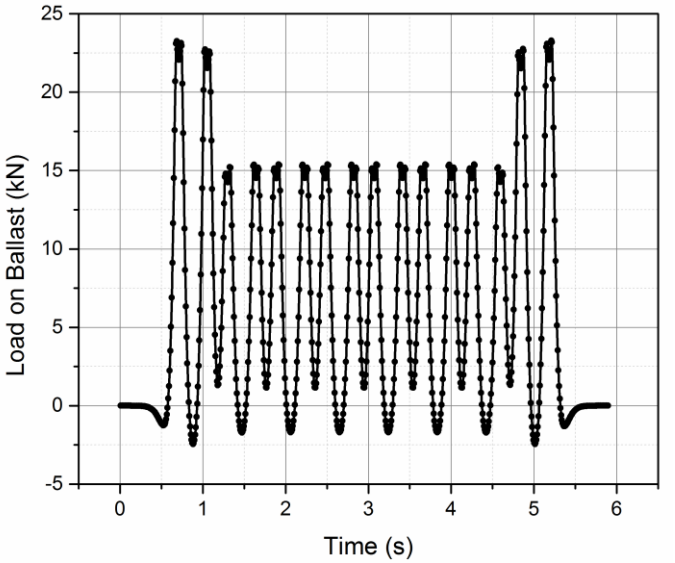

Figure 5. Load Levels Applied on the Ballast Layer as Predicted by the Fully Coupled 3-Dimensional Dynamic Track Model

4 IMAGING AIDED DISCRETE ELEMENT MODELING OF RAILROAD TRACK SECTIONS

The load levels on top of the ballast layer as predicted by the dynamic track model, were used as input in an imaging aided discrete element method (DEM) to predict the ballast layer behavior. The image-aided DEM simulation approach developed at the University of Illinois has the capability to create actual ballast aggregate particles as three-dimensional polyhedron elements having the same particle size distributions and imaging quantified average shapes and angularities. Ghaboussi and Barbosa (1990) developed the first polyhedral 3D DEM code BLOKS3D for particle flow; and Nezami et al. (2006) enhanced the program with new, fast contact detection algorithms. Tutumluer et al. (2006) combined the DEM program and the aggregate image analysis together to simulate the ballast behavior more accurately and realistically by using polyhedral elements regenerated from the image analysis results of ballast materials. This DEM approach was first calibrated by laboratory large scale direct shear test results for ballast size aggregate application (Huang & Tutumluer 2011). The calibrated DEM model was then utilized to model strength and settlement behavior of railroad ballast for the effects of multi-scale aggregate morphological properties (Tutumluer et al. 2006, 2007). A successful field validation study was also conducted with the ballast DEM simulation approach through constructing and monitoring field settlement records of four different ballast test sections and then comparing the measured ballast settlements under monitored train loadings to DEM model predictions (Tutumluer et al. 2011).

The first step in this process involved collecting representative ballast materials from the instrumented bridge approaches. The particle size distribution of the ballast was first established in the laboratory through sieving, and have been presented in Figure 6. The ballast material corresponded to AREMA # 3 gradation. Besides sieving, ballast particles corresponding to different sieve sizes were also scanned using the University of Illinois Aggregate Image Analyzer (UIAIA) to establish imagine-based particle morphological indices such as Angularity Index (Rao et al., 2002), Flat & Elongated Ratio (Rao et al., 2001), and Surface Texture Index. The average values for these imaging based morphological indices were found to be 384, 2.2, and 1.4, respectively.

These morphological indices were subsequently used to select representative polyhedral ballast particles to constitute the track model using a discrete element program (BLOKS3D) developed at the University of Illinois. Figure 7 shows the dimensions of the half-track model generated using the BLOKS3D program, used in this study.

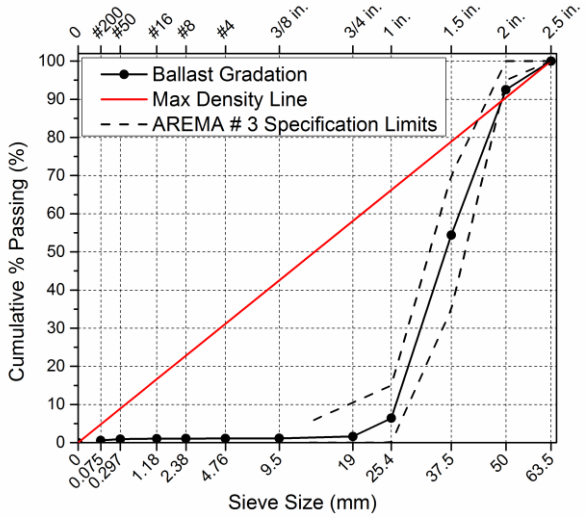

Figure 6: Particle Size Distribution of Ballast Material Used on Site

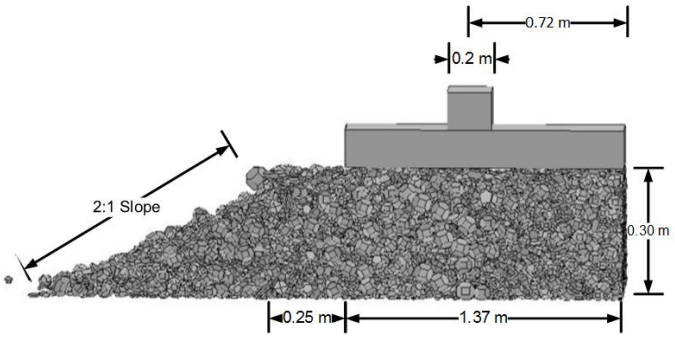

Figure 7. Half Track Model Generated Using Discrete Element Method

Different steps followed to create the half-track model using the BLOKS3D program are listed below: (1) Create a particle library to match the aggregate morphological properties established through image analysis; (2) Drop the particles to form a cuboid section; (3) Compaction Stage I: Use one top platen to compact the ballast particles by pressing downwards; all the side and bottom boundaries simulated as rigid during this stage; (4) Release the rigid boundary on the left hand side of the model to form the ballast shoulder slope; (5) Compaction Stage II: Use one top platen and one side platen (on a 2:1 slope) to compact the section without changing its shape; (6) Delete the compaction platens and extra particles from the model; (7) Set the tie and rail on top of the compacted ballast layer at the appropriate location; (8) Modify the boundary properties to have the same contact stiffness as the ballast to ballast particle contact; (9) Apply the load history determined from the analytical track model.

It is important to note that the boundary immediately underneath the ballast layer was also assigned a stiffness value equal to the inter-particle contact stiffness. Accordingly, the boundary underneath the ballast layer is rigid, and undeformable. Accordingly, the primary area of interest for the DEM modeling approach is the individual particle behavior within the ballast layer. The acceleration time histories for individual ballast particles at different positions along within the ballast layers were monitored, and inferences regarding the layer behavior were drawn.

5 RESULTS AND DISCUSSION

Figure 8 presents individual ballast particle acceleration levels determined at different positions within the ballast layer using the BLOKS3D program. As shown in the figure, the acceleration levels imposed on individual ballast particles under train loading can be significantly different depending on the position of the ballast particle with respect to the load position.

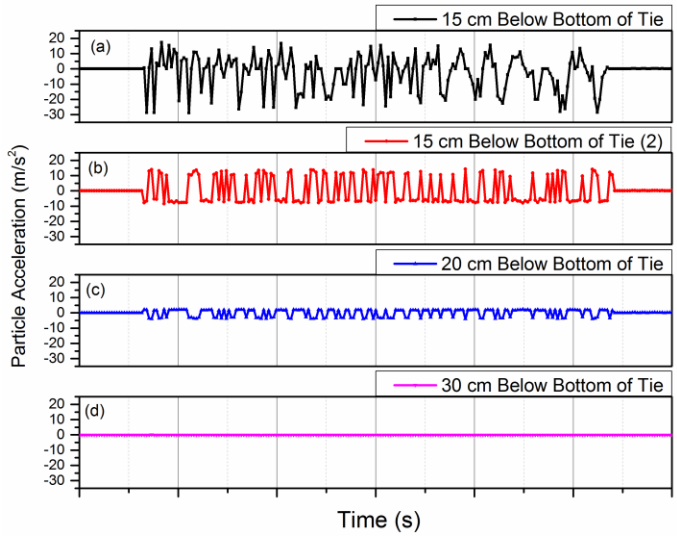

Figure 8. Comparing the Particle Acceleration Levels at Different Positions within the Ballast Layer: (a) 15 cm below bottom of tie: Position 1; (b) 15 cm below bottom of tie: Position 2; (c) 20 cm below bottom of tie; (d) 30 cm below bottom of tie

Two important observations can be made from the data presented in Figure 8. Firstly, the acceleration levels for the individual particles reduces significantly as the distance of the particle increases from the bottom of the tie. Accordingly, the acceleration levels observed for a particle 30 cm below the bottom of the tie (Figure 8-d) is significantly lower than particles located 15 cm below the bottom of the tie (see Figure 8-a and 8-b). Secondly, the particle acceleration can change significantly with lateral position, even at the same depth from the bottom of the tie. This is clearly apparent from comparing Figure 8-a, and 8-b. Although both these particles are at the same level (15 cm below the bottom of the tie), the acceleration time histories for both the particles are clearly different from each other. This difference can be attributed to the mechanism of load transfer within a particulate layer. As discussed by Oda (1974) and Tutumluer (1995), the load transfer within a granular material is usually along a continuous column of particles. Accordingly, the acceleration induced on an individual particle is largely dependent on its position with respect to the load transfer column.

Particles between the load transfer columns only provide lateral support, but do not carry much load. Therefore, the vertical accelerations induced in these particles is significantly lower compared to those lying directly along the load transfer columns. The particle corresponding to the acceleration levels reported in Figure 8-a lies directly along the load transfer column, therefore showing distinctive peaks with corresponding to each load pulse. However, the particle represented in Figure 8-b lies adjacent to the load transfer column, resulting in lower peaks corre-

sponding to each load pulse. Similarly, the acceleration values gradually decrease as the distance of a particle from the load transfer column is increased. A similar decrease in particle acceleration values is noticed as the vertical distance from the bottom of the tie is increased. The acceleration values approach zero at a distance of 30 cm form the bottom of the tie.

From the above reported results, it is evident that particle acceleration values within a ballast layer can be significantly different depending on the location of the ballast particle with respect to the load position. Using one acceleration value for the entire layer is therefore erroneous, and can be misleading as far characterizing the dynamic behavior of individual layers is concerned. This highlights a major shortcoming of analysis approaches based on the principles of finite element, or finite difference methods that characterize the ballast layer as one continuum, and assign one acceleration value to the entire layer.

6 LIMITATIONS OF THE INTEGRATED APPROACH IN ITS CURRENT FORM

Although the integrated approach presented in this paper marks a significant improvement over continuum based approaches, its current implementation has the following limitations:

1 The top LVDT was installed within the concrete crosstie just above the top of the ballast layer. Therefore, non-uniform support conditions underneath the crosstie can lead to different displacement time histories for the crosstie and the ballast layer.

2 The current implementation of the dynamic track model reported in this paper does not account for missing and/or disintegrated ties. Consideration of the missing and/or disintegrated ties can lead to a different load time history on top of the ballast layer, thus changing the results reported in this paper.

3 The boundary immediately underneath the ballast layer has been modeled as non-deformable within the BLOKS3D program. This may potentially lead to different damping characteristics near the bottom boundary, thus affecting the predicted acceleration values.

4 Particle acceleration values reported in this paper have been obtained from only one simulation run. Repeated simulations using the BLOKS3D program should be performed to account for different initial conditions during the ballast layer compaction.

5 Particle accelerations reported in this paper need to be verified through additional instrumentation comprising the placement of accelerometers at different positions within the ballast layer.

7 SUMMARY AND CONCLUSIONS

This paper presented an integrated approach to dynamic analysis of railway track transitions through combined application of field instrumentation along with analytical and numerical modeling. The following conclusions can be drawn from results presented in this paper:

1 Particle accelerations within a granular medium is largely dependent on the relative position of an individual particle with respect to the load position.

2 Characterizing the ballast layer as a continuum and assigning one acceleration value to the entire layer may lead to erroneous predictions of dynamic track behavior.

8 ACKNOWLEDGEMENTS

The authors would like to acknowledge the efforts of Mr. Yin Gao, graduate student at the Pennsylvania State University, and Mr. Huseyin Boler, graduate student at the University of Illinois for their help with the analytical modeling and data analyses efforts. The help of Mike Tomas, Marty Perkins, and Carl Walker of AMTRAK, Hasan Kazmee, Mike Wnek, and James Pforr of University of Illinois during the field instrumentation efforts is greatly appreciated. Field instrumentation data reported in this paper were collected under the scope of an ongoing research study at the University of Illinois, titled “Mitigation of Differential Movement at Railway Transitions for US High Speed Passenger Rail and Joint Passenger/Freight Corridors”. The authors acknowledge the contributions of Prof. Timothy D. Stark and Dr. James P. Hyslip for their assistance in the above mentioned research project.

REFERENCES

DeBeer, M., E. Horak, and A. Visser. 1989. The Multidepth Deflectometer (MDD) System for Determining the Effective Elastic Moduli of Pavement Layers. *Nondestructive Testing of Pavements and Backcalculation of Moduli*, ASTM STP, Vol. 1026pp. 70–89.

Ghaboussi J. and R. Barbosa. 1990. Three-dimensional Discrete Element Method for Granular Materials. *International Journal for Numerical and Analytical Methods in Geomechanics*, Vol. 14 (7): 451-472

Gräbe, P. J., C. Clayton, and F. J. Shaw. 2005. Deformation Measurement on A Heavy Haul Track Formation. *Presented at the Eighth International Heavy Haul Conference*, 2005.

Gräbe, P. J., and F. J. Shaw. 2010. Design Life Prediction of a Heavy Haul Track Foundation. *Proceedings of the Institution of Mechanical Engineers, Part F: Journal of Rail and Rapid Transit*, Vol. 224(5): 337–344.

Huang, H., S. Shen, and E. Tutumluer. 2010. Moving Load on Track with Asphalt Trackbed. *Journal of Vehicle System Dynamics*. Vol. 48(6): 737-749.

Huang H., and Tutumluer E. (2011). Discrete Element Modeling for Fouled Railroad Ballast. *Construction and Building Materials* 25 (8): 3306–3312

Huang, H., Y. Gao, and S. Stoffels. 2013. A Fully Coupled 3D Train-Track-Soil Model for High Speed Rail. *Submitted for Presentation and Publication at the 93rd Annual Meeting of the Transportation Research Board, January, 2014*.

Mishra, D., E. Tutumluer, T. D. Stark, J. P. Hyslip, S. M. Chrismer, and M. Tomas. 2012. Investigation of Differential Movement at Railroad Bridge Approaches through Geotechnical Instrumentation. *Journal of Zhejiang University SCIENCE A*, Vol. 13(11): 814–824.

Nezami E. G., Y. M. A. Hashash, D. Zhao, and J. Ghaboussi. 2006. Shortest Link Method for Contact Detection in Discrete Element Method. *International Journal for Numerical and Analytical Methods in Geomechanics*, 30(8): 783-801

Oda, M. 1974. A Mechanical and Statistical Model of Granular Materials. *Soils and Foundations*, Vol. 14, Japanese Society of Soil Mechanics and Foundation Engineering.

Priest, J. A., W. Powrie, L. Yang, P. J. Gräbe, and C. R. I. Clayton. 2010. Measurements of Transient Ground Movements below a Ballasted Railway Line. *Géotechnique*, Vol. 60(9): 667–677.

Rao, C., E. Tutumluer, and J.A. Stefanski. 2001. Flat and Elongated Ratios and Gradation of Coarse Aggregates Using a New Image Analyzer. ASTM Journal of Testing and Standard, 29(5):79-89.

Rao, C., E. Tutumluer, and I.T. Kim (2002). Quantification of Coarse Aggregate Angularity Based on Image Analysis. Transportation Research Record: Journal of the Transportation Research Board. No. 1787: 193-201.

Scullion, T., B. R, and L. R. 1989. Using the Multidepth Deflectometer to Verify Modulus Backcalculation Procedures. *Nondestructive Testing of Pavements and Backcalculation of Moduli*, ASTM STP, Vol. 1026: 90–101.

Tutumluer, E. 1995. Predicting Behavior of Flexible Pavements with Granular Bases. Ph.D. Thesis. Department of Civil Engineering, Georgia Institute of Technology.

Tutumluer, E., H. Huang, Y. M. A. Hashash, and J. Ghaboussi. 2006. Aggregate Shape Effects on Ballast Tamping and Railroad Track Lateral Stability. *In Proceedings of the AREMA Annual Conference*, Louisville, Kentucky, USA, September 17-20.

Tutumluer, E., H. Huang, Y. M. A. Hashash, and J. Ghaboussi. 2007. Discrete Element Modeling of Railroad Ballast Settlement. *In Proceedings of the AREMA Annual Conference*, Chicago, Illinois, September 9-12.

Tutumluer, E., Y. Qian, Y. M. A. Hashash, J. Ghaboussi, J., and D. D. Davis. 2011. Field Validated Discrete Element Model for Railroad Ballast. *In Proceedings of the AREMA Annual Conference*, Minneapolis, Minnesota, September 18-21.

Vorster, D. J., and P. J. Gräbe. 2013. The Effect of Axle Load on Track and Foundation Resilient Deformation under Heavy Haul Conditions. *Presented at the 10th International Heavy Haul Association Conference*, New Delhi, India.